Magnetic reversal in $Sr_4Ru_3O_{10}$ nanosheets probed by anisotropic magnetoresistance

Yan Liu,[1,2] Weiwei Chu,[2] Jiyong Yang,[2,*] Guoqiang Liu,[3] Haifeng Du,[2] Wei Ning,[2] Langsheng Ling,[2] Wei Tong,[2] Zhe Qu,[2] Gang Cao,[4] Zhuan Xu,[1,5] and Mingliang Tian[2,5,†]

[1]*State Key Laboratory of Silicon Materials and Department of Physics, Zhejiang University, Hangzhou 310027, China*

[2]*Anhui Province Key Laboratory of Condensed Matter Physics at Extreme Conditions, High Magnetic Field Laboratory, Chinese Academy of Sciences, Hefei 230031, Anhui, China*

[3]*Ningbo Institute of Material Technology and Engineering, Chinese Academy of Sciences, Ningbo 315201, China*

[4]*Department of Physics, University of Colorado at Boulder, Boulder, Colorado 80309, USA*

[5]*Collaborative Innovation Center of Advanced Microstructures, Nanjing University, Nanjing 210093, China*

(Received 16 March 2018; revised manuscript received 20 June 2018; published 25 July 2018)

The origin of the unusual second magnetic transition at a temperature T_M in the ruthenate $Sr_4Ru_3O_{10}$ remains elusive. Here, we have investigated the thickness-dependent anisotropic magnetoresistance of $Sr_4Ru_3O_{10}$ nanosheets, and clearly found that the sign of the magnetoresistance (MR) presents an unusual reversal behavior from a positive to negative with an external magnetic field $H \perp ab$ plane or vice versa with $H \parallel ab$ plane when the temperature decreases across the T_M. Analysis of the data demonstrates that this MR reversal is caused by the magnetization reversal from the ab plane ferromagnetic order at $T > T_M$ to the c direction at $T < T_M$ due to the competition between the shape anisotropy and the inherent magnetocrystalline anisotropy. Our result suggests that the second magnetic transition in $Sr_4Ru_3O_{10}$ nanosheets originates from a spin reorientation.

DOI: 10.1103/PhysRevB.98.024425

I. INTRODUCTION

Layered perovskite $4d$ ruthenates $Sr_{n+1}Ru_nO_{3n+1}$ ($n = 1, 2, \infty$), in which the spin and orbit or lattice are strongly coupled, are attractive materials in condensed matter physics [1]. First, this series contains novel phenomena, including spin-triplet superconductivity [2] and quantum criticality [3,4]. Second, the physical property in this series is highly tunable by external excitations such as strain and magnetic field [5–8]. Third, as n increases, the magnetism evolves systemically from paramagnetism (Sr_2RuO_4, $n = 1$) [9], enhanced paramagnetism ($Sr_3Ru_2O_7$, $n = 2$) [6] to ferromagnetism ($SrRuO_3$, $n = \infty$) [10].

The triple-layer $Sr_4Ru_3O_{10}$ ($n = 3$) is a ferromagnetic (FM) metal with a Curie temperature $T_C \sim 105$ K [11,12]. Its FM transition is followed by a second magnetic transition at a critical temperature T_M of 50–70 K, accompanied by a resistive anomaly in transport measurements [11–16]. Below T_M, its magnetization shows an additional increase when the magnetic field (H) is applied parallel to the c axis ($H \parallel c$), whereas the magnetization decreases gradually to near zero for $H \parallel ab$ plane [11,12]. However, specific-heat measurements show no anomaly near T_M, suggesting that the second transition might be not a real thermodynamic phase transition [17]. The origin of this transition is still controversial and remains elusive [18–24]. For example, an early Raman study suggested that at $T_M < T < T_C$, the magnetic moments are canted and FM aligned along the c axis with no ordering of the in-plane component, whereas at $T < T_M$, the in-plane component of the moments are antiferromagnetically coupled [18]. However, a neutron diffraction measurement performed by Granata *et al.* [23] showed that at zero field below T_C, the magnetic moments are FM-coupled and oriented along the c axis with neither long-range antiferromagnetic nor FM order in the ab plane. On the other hand, a very recent neutron diffraction study performed by Zhu *et al.* [24] showed that the magnetic moments are FM coupled with both in-plane and out-of-plane FM components, and below T_M, the magnetic moments incline continuously toward the out-of-plane direction.

Recently, we have studied the transport property of $Sr_4Ru_3O_{10}$ nanosheets. Three unusual features were observed: (i) The T_M decreases with decreasing thickness (see also in Fig. 1) [20]; (ii) there is an in-plane FM order along the [110] direction below T_C probed by the planar Hall effect [21,22]; and (iii) the domain structure of the in-plane FM order in the nanosheet (lateral size: $< 10\,\mu$m) transforms from a single-domain state at $T > T_M$ into a multidomain state at $T < T_M$ [21]. These findings open a path to explore the nature of the second transition by using thickness as a control parameter.

In this paper, we performed a systematically anisotropic magnetoresistance (AMR) study on high quality $Sr_4Ru_3O_{10}$ nanosheets with different thicknesses. We found that the sign of the magnetoresistance (MR) in nanosheets presents a clear "reversal" behavior from a positive to negative when the temperature is varied across the critical point T_M, no matter whether the magnetic field is applied along the c axis or the ab plane. These results indicate that there is a spin reorientation process at T_M in $Sr_4Ru_3O_{10}$ nanosheets.

II. EXPERIMENTAL DETAILS

$Sr_4Ru_3O_{10}$ nanosheets were obtained by the scotch-tape-based micromechanical exfoliation method from the bulk single crystal grown by flux techniques [11]. The nanosheets

*jyyang@hmfl.ac.cn
†tianml@hmfl.ac.cn

with different thicknesses, d, determined by atomic force microscopy were transferred to a silicon substrate covered with 300-nm-thick silicon dioxide on the top surface. Contacts were patterned using an electron-beam lithography technique followed by deposition of Ti/Au (5 nm/100 nm). A standard four-probe configuration was used to carry out the transport measurements, with the current is injected in the ab plane.

III. RESULTS AND DISCUSSION

Figure 1 shows a typical resistance (R) versus temperature (T) curve and its derivative dR/dT (right axis) of a 25-nm-thick $Sr_4Ru_3O_{10}$ nanosheet, both anomalies (see more clearly in the dR/dT curve) in R are indicated by arrows, at which the temperatures are, respectively, defined as T_C and T_M. It is noted that (i) The nanosheets used in this paper exhibit a similar R-T property as that of the bulk [13], except for the decrease of the second resistive anomaly temperature T_M due to the size effect; (ii) the residual resistance ratio, $RRR = R(300\,\mathrm{K})/R(2\,\mathrm{K})$, reaches about 60; and (iii) the residual resistivity at 2 K is about 2–4 $\mu\Omega$ cm, which is comparable to that of the bulk $Sr_4Ru_3O_{10}$ crystals grown by the floating-zone technique (e.g., 1.6 $\mu\Omega$ cm in Ref. [13]). All these results indicate that our nanosheets are of high quality, and the possible intergrowth phases such as $Sr_3Ru_2O_7$ [6] and $SrRuO_3$ [10], which are usually seen in bulk crystals grown by the flux method, can be ruled out, as these phases will present completely different R-T properties compared with $Sr_4Ru_3O_{10}$. The thickness dependence of both T_C and T_M are presented in the inset of Fig. 1. It can be seen that the T_C is almost independent on the variations of the thickness (i.e., even when the thickness is reduced to 25 nm) and remains at ~105 K as in the bulk. The T_M, however, is affected significantly by the thickness and decreases to ~25 K, which is almost the half value of the bulk as the thickness is reduced to less than ~100 nm.

Figure 2 shows the R-H curves of three samples with thickness, 25, 89, and 260 nm, respectively, at $T = 70$ and 15 K. It is clearly seen that, at $T = 70\,\mathrm{K}$ ($> T_M$) [see Figs. 2(a), 2(c), and 2(e)], all the R-H curves present a "valley" shape with a positive MR at low fields when the field H is applied perpendicular to the ab plane (i.e., $H \perp ab$), whereas a "cusp" with negative MR in the parallel field direction (i.e., $H \parallel ab$). Interestingly, when the temperature is at 15 K ($< T_M$) [see Figs. 2(b), 2(d), and 2(f)], the R-H properties present a completely opposite behavior except for the hysteresis, i.e., a cusp with negative MR for $H \perp ab$ but a valley with positive MR for $H \parallel ab$.

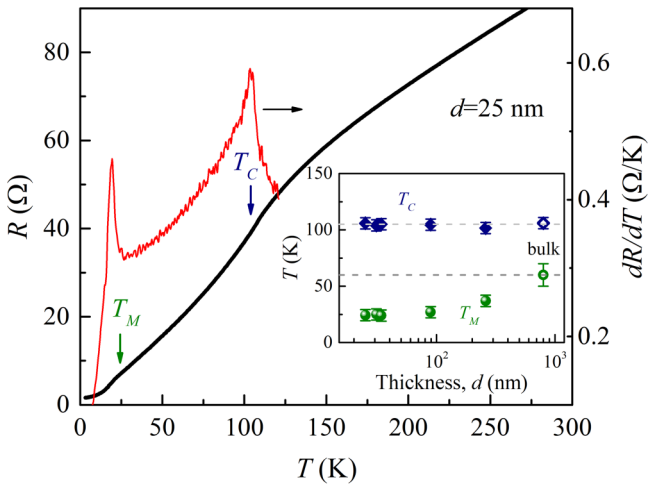

FIG. 1. $R-T$ and its derivative dR/dT (right axis) at zero field of a 25 nm-thick $Sr_4Ru_3O_{10}$ nanosheet. Temperatures T_C and T_M are indicated by arrows. Inset: Temperature-dependent T_C and T_M of different-thickness $Sr_4Ru_3O_{10}$ nanosheets.

In order to understand this unusual MR reversal behavior by changing the polarization direction of the external magnetic field, we first consider the principle of the AMR effect in a magnetic system. Generally, in a FM metal, the AMR effect resulting from the spin-orbit coupling can be written as [25]

$$R = R_p - (R_p - R_{\mathrm{perp}})\sin^2\theta, \tag{1}$$

where R_p and R_{perp} are, respectively, the resistance for the current oriented parallel and perpendicular to the magnetization, and θ is the angle between the magnetization M and current. When H is applied perpendicular to the direction of magnetization and its value is less than the saturation field, θ is determined by $\sin\theta = H/M_s$ (M_s is the saturation magnetization) due to a rotation of M against the demagnetizing field [25]. In this case, Eq. (1) predicts a parabolic behavior of the resistance with H, i.e., a valley in MR. Therefore, the observed valley in MR as demonstrated in Fig. 2 for $H < H_s^{\perp}$ at 70 K (or $H < H_s^{\parallel}$ at 15 K) is mainly a result of demagnetization effects. Here, $H_s^{\perp}$ and $H_s^{\parallel}$ are, respectively, the saturation fields for $H \perp ab$ and $H \parallel ab$ as marked in Figs. 2(e) and 2(f). The fact that the parabolic behavior appears at 70 K in $H \perp ab$ implies that the magnetization in the nanosheet is predominantly oriented in the ab plane at 70 K, which is consistent with our previous planar Hall effect study [21]; the negative MR with a cusp shape at 70 K with $H \parallel ab$ is also a typical feature for an in-plane FM metal. Similarly, the parabolic MR behavior observed at 15 K with $H \parallel ab$ indicates that the magnetization should be oriented along the c direction, verified by the negative MR behavior with a cusp shape when the field H is perpendicular to the ab plane. In other words, there must be a magnetic reversal from an in-plane FM order to the c direction when the temperature decreases from above.

To determine the critical temperature for the reversal, we have measured the MR behavior for $H \parallel ab$ and $H \perp ab$ as a function of temperatures in nanosheets with different thicknesses. Figure 3 shows the MR behavior obtained in a 260-nm-thick sample, where the saturation fields of the valley are indicated by arrows. One can see that no matter whether the field is applied with $H \parallel ab$ [Fig. 3(a)] or $H \perp ab$ [Fig. 3(b)], a striking feature is that the MR always presents a reversal at a temperature between 35 and 40 K. For example, the R-H curves with $H \perp ab$ (or $H \parallel ab$) show a valley (or cusp) with positive (or negative) MR above ~37 K, then transition to a cusp (or valley) with negative (or positive) MR, and the reversal temperature, ~37 K, is consistent with the second anomaly temperature, $T_M \sim 37$ K of the nanosheet defined from the R-T curve (inset of Fig. 1). This result indicates the T_M itself is a critical energy scale of the magnetization reversal. In other words, above T_M the magnetic moments prefer to be FM aligned in the ab plane (along the [110]

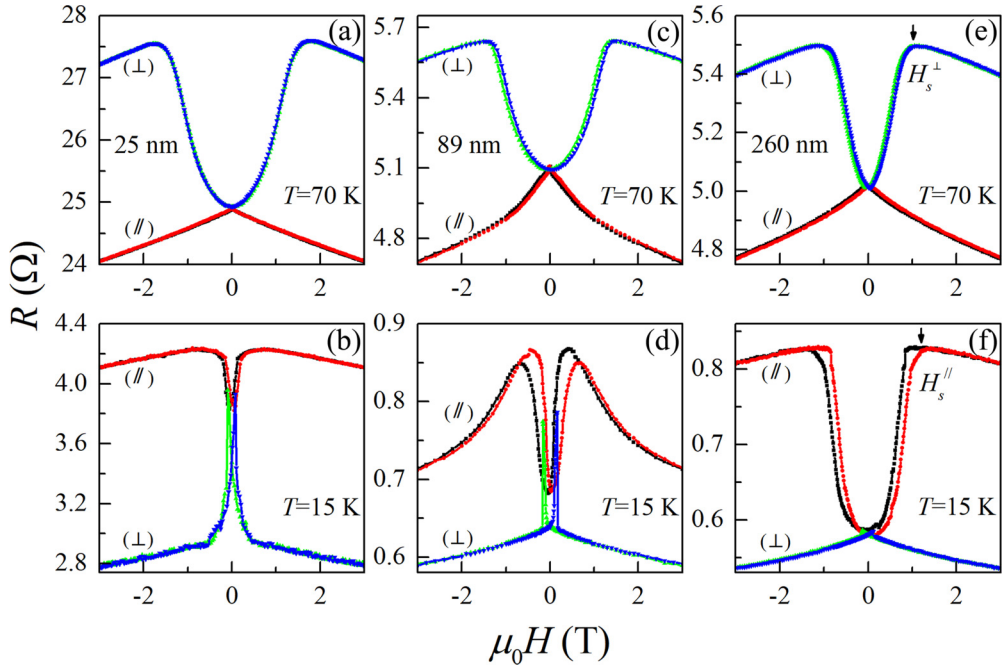

FIG. 2. Magnetoresistance of different-thickness $Sr_4Ru_3O_{10}$ nanosheets at 70 and 15 K. (a) and (b) 25 nm; (c) and (d) 89 nm; (e) and (f) 260 nm. The superscript ⊥ (∥) indicates the magnetic field is applied perpendicular (parallel) to the ab plane, and $H_s^{\perp}$ ($H_s^{\parallel}$) is the saturation field for $H \perp ab$ ($H \parallel ab$).

direction [21,22]), whereas below T_M the moments turn mostly to the c axis, as schematically shown in Fig. 4(a). This is also

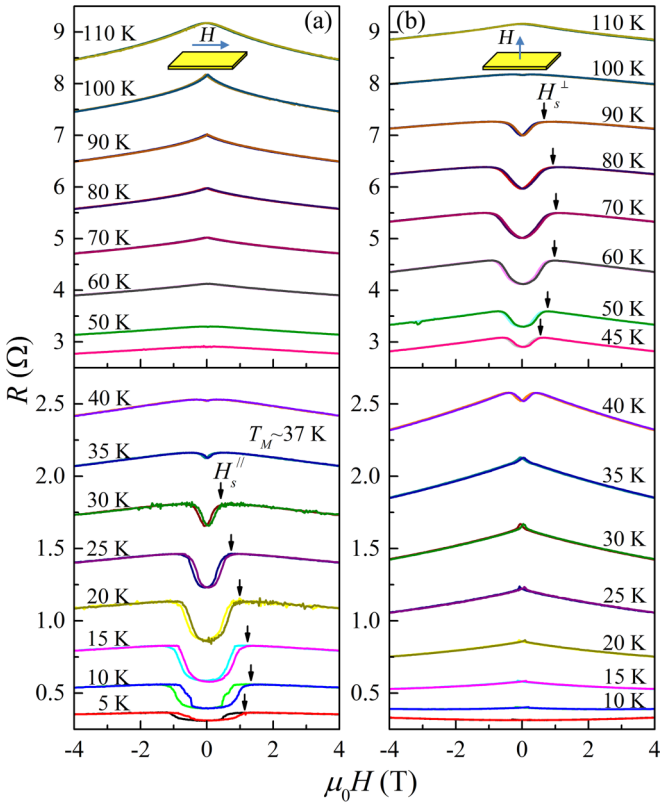

FIG. 3. Magnetic field H-dependent resistance as a function of temperatures in a 260-nm-thick $Sr_4Ru_3O_{10}$ nanosheet. (a) $H \parallel ab$; (b) $H \perp ab$.

partially supported by the fact that the in-plane FM order in the $Sr_4Ru_3O_{10}$ nanosheet transforms from a single-domain state at $T > T_M$ into a multidomain state at $T < T_M$ demonstrated in our previous work [21]. Based on this finding, the origin of the second resistive anomaly, i.e., the second transition at T_M in the $Sr_4Ru_3O_{10}$ nanosheet (Fig. 1) is well understood, which is actually caused by the spin rotation from in-plane to out-of-plane order.

Evidently, there are competing sources for the magnetization reversal. In $Sr_4Ru_3O_{10}$ bulk, it has been found that the Ru moments are primarily FM-coupled along the c axis below T_C [12,23,24], so the fact that the magnetization is predominantly oriented along the ab plane at $T_M < T < T_C$ in nanosheets [Fig. 4(a)] must have an origin due to the size effect, i.e., the shape anisotropy. Therefore, a natural question is what factor will overcome the existing size effect and drive the moments back to the c axis below T_M in the nanosheet?

To give an insight on this question, we summarize the saturation fields $H_s^{\parallel}$ and $H_s^{\perp}$ of different-thickness samples as a function of temperature in Fig. 4(b), where the valley-shaped MR can be seen only above T_M for $H \perp ab$ (or below T_M for $H \parallel ab$) as shown in Fig. 3. Both the saturation fields, $H_s^{\parallel}$ and $H_s^{\perp}$, are crucial factors to characterize how difficult it is to polarize the moments. It was found that the $H_s^{\perp}$ in the temperature range of $T > T_M$ increases as the thickness decreases, whereas the $H_s^{\parallel}$ in the temperature range of $T < T_M$ decreases correspondingly, clearly demonstrating that thinner samples favor spins aligned in the ab plane due to the size effect. However, the variation of both $H_s^{\perp}$ and $H_s^{\parallel}$ for different-thickness samples presents a similar profile with T, namely a maximum near ~70 K (in the vicinity of the bulk T_M, e.g., Refs. [13–15]) for $H_s^{\perp}$ and ~10 K for $H_s^{\parallel}$, indicating there must be an intrinsic origin beyond the shape anisotropy that

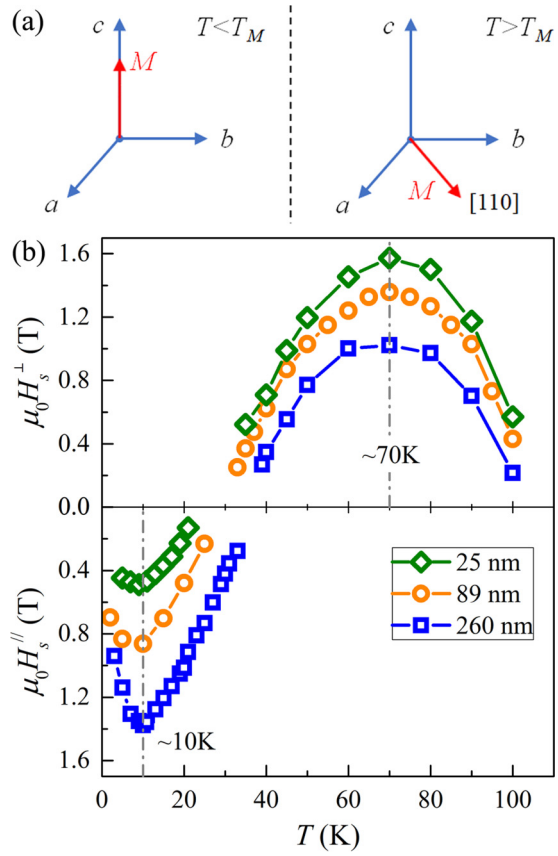

FIG. 4. (a) Schematic plot of the magnetization M of the $Sr_4Ru_3O_{10}$ nanosheet below T_C. (b) Temperature-dependent saturation fields $H_s^{\perp}$ and $H_s^{\parallel}$ of different-thickness nanosheets extracted from R-H curves.

modulates the spin reorientation from the in-plane order to the c axis.

It is known that there are unique magnetic and structural responses of $Sr_4Ru_3O_{10}$ under an external magnetic field [18,23]. The T-dependent $H_s^{\perp}$ and $H_s^{\parallel}$ might be crystal structure related, for the profile of which is less reliant on the thickness. Indeed, by carefully reviewing the structure of $Sr_4Ru_3O_{10}$ upon cooling [23,26], we find both $H_s^{\perp}$ and $H_s^{\parallel}$ in nanosheets follow the evolution of the lattice parameter c. Specifically, the increase of $H_s^{\perp}$ corresponds to the decrease of c from T_C to ~70 K, and when c expands from ~70 K to 15 K (the lowest temperature achieved in the structural measurements [23,26]), the $H_s^{\perp}$ goes to zero at T_M, and there is a monotonous increase of $H_s^{\parallel}$ [Fig. 4(b)]. We conclude that the observed magnetic structure in nanosheets [Fig. 4(a)] actually arises from the competition between the shape anisotropy and the magnetocrystalline anisotropy, where the shape anisotropy favors the magnetic moment in the ab plane, whereas the magnetocrystalline anisotropy, which can be enhanced significantly by the expansion of the c axis below 70 K, favors the moment aligning along the c direction. This strongly structure-related magnetocrystalline anisotropy is intrinsic, which is independent on the thickness of samples. Our speculation is consistent with the theoretical prediction [27,28] that the elongated (flattened) RuO_6 octahedra favor the magnetic moments arranged along the c direction (ab plane). Below ~70 K (i.e., the maximum in $H_s^{\perp}$), an expansion of c induces a continuous enhancement of the magnetocrystalline anisotropy energy, and finally overcomes the shape anisotropy below T_M, thus leading to a magnetic reversal from the in-plane FM order to the c direction. The shape anisotropy increases as the thickness decreases, which is why the T_M in nanosheets exhibits a thickness-dependent property as shown in the inset of Fig. 1. The origin of the T_M in nanosheets is consistent with the recent neutron diffraction data on bulk crystals obtained by Zhu *et al.* [24], where below $T_M \sim 50$ K, the magnetic moments incline continuously toward the out-of-plane direction, and at $T = 1.5$ K, the spins are nearly aligned along the c axis. The significant difference between a bulk and nanosheet is that the FM component in the ab plane of a bulk sample is weak due to the lack of shape anisotropy. It is worth mentioning here that the overall expansion of c from ~70 K down to 15 K is only $\sim 4 \times 10^{-4}$ [26], but it is large enough to overcome the shape anisotropy and drive the direction of magnetization back to the c axis. The turning point at ~10 K (i.e., the maximum in $H_s^{\parallel}$) suggests another decrease of c, but it requires further low-temperature structural verification.

IV. SUMMARY

We have investigated the MR effect with H both parallel and perpendicular to the ab plane of $Sr_4Ru_3O_{10}$ nanosheets, and clearly observed a reversal behavior of the MR at T_M, i.e., a magnetization reversal from the ab plane at $T > T_M$ to the c direction at $T < T_M$. Analysis of the data demonstrates that this reversal of the MR profile is a result of the competition between the shape anisotropy and the inherent magnetocrystalline anisotropy. Our result can naturally explain the second magnetic transition at T_M in $Sr_4Ru_3O_{10}$ nanosheets, which is actually a spin reorientation transition.

ACKNOWLEDGMENTS

This work was supported by the National Key R&D Projects of China (Grant No. 2016FYA0300402), the National Natural Science Foundation of China (Grants No. 11674323, No. U1432251, No. 11774352, No. 11774305, and No. U1532153), the support of China Postdoctoral Science Foundation funded project (Grant No. 2018M632445), the program of Users with Excellence, the Hefei Science Center of CAS, and the CAS/SAFEA international partnership program for creative research teams of China.

[1] G. Cao, and L. Delong, *Frontiers of 4d- and 5d Transition Metal Oxides* (World Scientific Publishing, Singapore, 2013).

[2] K. Ishida, H. Mukuda, Y. Kitaoka, K. Asayama, Z.Q. Mao, Y. Mori, and Y. Maeno, Nature(London) **396**, 658 (1998).

[3] S. A. Grigera, R. S. Perry, A. J. Schofield, M. Chiao, S. R. Julian, G. G. Lonzarich, S. I. Ikeda, Y. Maeno, A. J. Millis, and A. P. Mackenzie, Science **294**, 329 (2001).
[4] R. S. Perry, L. M. Galvin, S. A. Grigera, L. Capogna, A. J. Schofield, A. P. Mackenzie, M. Chiao, S. R. Julian, S. I. Ikeda, S. Nakatsuji, Y. Maeno, and C. Pfleiderer, Phys. Rev. Lett. **86**, 2661 (2001).
[5] C. W. Hicks, D. O. Brodsky, E. A. Yelland, A. S. Gibbs, J. A. N. Bruin, M. E. Barber, S. D. Edkins, K. Nishimura, S. Yonezawa, and Y. Maeno, and A. P. Mackenzie, Science **344**, 283 (2014).
[6] S. I. Ikeda, Y. Maeno, S. Nakatsuji, M. Kosaka, and Y. Uwatoko, Phys. Rev. B **62**, R6089(R) (2000).
[7] C. Lester, S. Ramos, R. S. Perry, T. P. Croft, R. I. Bewley, T. Guidi, P. Manuel, D. D. Khalyavin, E. M. Forgan, and S. M. Hayden, Nat. Mater. **14**, 373 (2015).
[8] D. O. Brodsky, M. E. Barber, J. A. N. Bruin, R. A. Borzi, S. A. Grigera, R. S. Perry, A. P. Mackenzie, and C. W. Hickey, Sci. Adv. **3**, e1501804 (2017).
[9] Y. Maeno, H. Hashimoto, K. Yoshida, S. Nishizaki, T. Fujita, J. G. Bednorz, and F. Lichtenberg, Nature(London) **372**, 532 (1994).
[10] G. Koster, L. Klein, W. Siemons, G. Rijnders, J. S. Dodge, C.-B. Eom, D. H. A. Blank, and M. R. Beasley, Rev. Mod. Phys. **84**, 253 (2012).
[11] M. K. Crawford, R. L. Harlow, W. Marshall, Z. Li, G. Cao, R. L. Lindstrom, Q. Huang, and J. W. Lynn, Phys. Rev. B **65**, 214412 (2002).
[12] G. Cao, L. Balicas, W. H. Song, Y. P. Sun, Y. Xin, V. A. Bondarenko, J. W. Brill, S. Parkin, and X. N. Lin, Phys. Rev. B **68**, 174409 (2003).
[13] Z. A. Xu, X. F. Xu, R. S. Freitas, Z. Y. Long, M. Zhou, D. Fobes, M. H. Fang, P. Schiffer, Z. Q. Mao, and Y. Liu, Phys. Rev. B **76**, 094405 (2007).
[14] E. Carleschi, B. P. Doyle, R. Fittipaldi, V. Granata, A. M. Strydom, M. Cuoco, and A. Vecchione, Phys. Rev. B **90**, 205120 (2014).
[15] Y. J. Jo, L. Balicas, N. Kikugawa, E. S. Choi, K. Storr, M. Zhou, and Z. Q. Mao, Phys. Rev. B **75**, 094413 (2007).
[16] F. Weickert, L. Civale, B. Maiorov, M. Jaime, M. B. Salamon, E. Carleschi, A. M. Strydom, R. Fittipaldi, V. Granata, and A. Vecchione, Sci. Rep. **7**, 3867 (2017).
[17] X. N. Lin, V. A. Bondarenko, G. Cao, and J. W. Brill, Solid State Commun. **130**, 151 (2004).
[18] R. Gupta, M. Kim, H. Barath, S. L. Cooper, and G. Cao, Phys. Rev. Lett. **96**, 067004 (2006).
[19] Z. Q. Mao, M. Zhou, J. Hooper, V. Golub, and C. J. O'Connor, Phys. Rev. Lett. **96**, 077205 (2006).
[20] Y. Liu, J. Y. Yang, W. K. Wang, H. F. Du, W. Ning, L. S. Ling, W. Tong, Z. Qu, Z. R. Yang, M. L. Tian, G. Cao, and Y. H. Zhang, New. J. Phys. **18**, 053019 (2016).
[21] Y. Liu, J. Y. Yang, W. K. Wang, H. F. Du, W. Ning, L. S. Ling, W. Tong, Z. Qu, G. Cao, Y. H. Zhang, and M. L. Tian, Phys. Rev. B **95**, 161103 (2017).
[22] Y. Liu, J. Y. Yang, W. W. Chu, H. F. Du, W. Ning, L. S. Ling, W. Tong, Z. Qu, G. Cao, Y. H. Zhang, and M. L. Tian, Appl. Phys. Lett. **111**, 033103 (2017).
[23] V. Granata, L. Capogna, M. Reehuis, R. Fittipaldi, B. Ouladdiaf, S. Pace, M. Cuoco, and A. Vecchione, J. Phys.: Condens. Matter **25**, 056004 (2013).
[24] M. Zhu, P. G. Li, Y. Wang, H. B. Cao, W. Tian, H. D. Zhang, B. D. Phelan, Z. Q. Mao, and X. Ke, Sci. Rep. **8**, 3914 (2018).
[25] E. D. Dahlberg, K. Riggs, and G. A. Prinz, J. Appl. Phys. **63**, 4270 (1988).
[26] W. Schottenhamel, M. Abdel-Hafiez, R. Fittipaldi, V. Granata, A. Vecchione, M. Hücker, A. U. B. Wolter, and B. Büchner, Phys. Rev. B **94**, 155154 (2016).
[27] M. Cuoco, F. Forte, and C. Noce, Phys. Rev. B **73**, 094428 (2006).
[28] V. Granata, L. Capogna, F. Forte, M. B. Lepetit, R. Fittipaldi, A. Stunault, M. Cuoco, and A. Vecchione, Phys. Rev. B **93**, 115128 (2016).